Energ. Ecol. Environ. (2023) 8(2):101–112
https://doi.org/10.1007/s40974-022-00264-3

ORIGINAL ARTICLE

Ibuprofen removal using activated carbon from acid-modified Acacia sawdust

Aila Jiezl R. Capistrano[1] · Rensel Jay D. Labadan[1] · Jan Earl B. Viernes[1] · Edison M. Aragua Jr.[1] · Rafael N. Palac[1] · Renato O. Arazo[1]

[1] College of Engineering and Technology, University of Science and Technology of Southern Philippines, 9004 Claveria, Philippines

Received: 20 July 2022 / Revised: 24 November 2022 / Accepted: 29 November 2022 / Published online: 12 December 2022

Abstract The concentration of non-steroid anti-inflammatory drugs like Ibuprofen in water bodies is alarming that may cause adverse effects on the aquatic ecosystem and human beings. This study investigated the removal of Ibuprofen in an aqueous solution using the acid-modified (phosphoric acid) Acacia sawdust activated carbon (ASAC). The ASAC underwent Scanning Electron Microscopy and Fourier Transform Infrared Spectroscopy analyses. The Ibuprofen (IBP) removal using ASAC was investigated in a batch experiment using a central composite design and considering the effects of adsorbent dose, contact time, and initial IBP concentration. Mechanisms that explained the adsorption of IBP onto ASAC were determined through isotherm and kinetic modeling. The findings revealed that the ASAC contained active site micropores and functional groups such as O–H, C–O, and COOH, which were responsible for adsorption via hydrogen and oxygen bonding between ASAC and IBP. The optimum IBP removal of 98.61% was attained at 0.20 g ASAC adsorbent dosage, 60 min contact time, and 400 ppm initial IBP concentration. The IBP compound was attached in the monolayer to the ASAC, with R^2 of 0.9787 of the Langmuir isotherm model. The physical attachment of IBP molecules onto the surface of ASAC via Van der Waals forces was known through the R^2 of 0.9863 of the pseudo-first-order kinetic model. Overall, the ASAC removed IBP from an aqueous solution with an adsorption capacity of 121.95 mg/g, suggesting its considerable potential as a novel source of activated carbon.

Keywords Acacia sawdust · Adsorption capacity · Langmuir isotherm · Pseudo-first-order kinetic · Central composite design

✉ Renato O. Arazo
roarazo@yahoo.com; renato.arazo@ustp.edu.ph

Aila Jiezl R. Capistrano
jiezlcaps@gmail.com

Rensel Jay D. Labadan
renzlabadan9102000@yahoo.com

Jan Earl B. Viernes
janearlviernes@gmail.com

Edison M. Aragua Jr.
nosidearagua@gmail.com

Rafael N. Palac
rafael.palac@ustp.edu.ph

1 Introduction

Wastes from pharmaceutical products are a worldwide concern due to their contribution to environmental pollution, particularly wastewater effluents (Rac et al. 2014). When not handled properly, the waste by-products in pharmaceuticals can adversely affect the water sources and pose a significant threat to human health and the environment (Ahmad et al. 2020b). This problem has been increasingly alarming due to its rampant use (Souza et al. 2021). One of the most profoundly used medicines produced by pharmaceutical industries is non-steroidal anti-inflammatory drugs (NSAID). Among the NSAIDs, Ibuprofen (IBP) is the most consumed worldwide, bringing emerging undesirable concentrations into water bodies affecting aquatic life and public health (Wang and Yang 2020). Some adverse effects are cell oxidative imbalance, changes in growth rate, reproduction, and behavior of various aquatic organisms (Chopra and Kumar 2020).

There are attempts to remove the presence of IBP in water, such as but not limited to: using electro-peroxide in carbon cloth filter with a 64.87% removal rate (Yang et al. 2020), modified chitosan at 33% removal efficiency (Phasuphan et al. 2019), and persulfate process with 85% removal (Oba et al. 2021a). Another known method of removing contaminants in the water is adsorption, a more advantageous process because it does not need sophisticated equipment and is easy to use. Using activated carbon as an adsorbent is the best option for removing pharmaceutical pollutants considering its unique characteristics such as high capacity and porosity (Ahmed 2017). A recent study has concentrated on employing agricultural wastes as adsorbents because these contain carbon chains, amine groups, and carboxyl and hydroxyl groups that can easily attach to the surface of pollutant ions (Solomon et al. 2020). Among the potential candidates as an adsorbent in removing contaminants in the water is Acacia sawdust, a waste by-product of the wood processing industry. The sawdust of Acacia has a desirable porous feature, high carbon content, and low ash content (Jamoussi et al. 2020), making it a promising precursor for producing activated carbon with higher efficiency in the removal of contaminants in wastewater (Oladimeji et al. 2021). In another study, Acacia sawdust was found to be among the top three most efficient biosorbent in the elimination of hazardous contaminants [Cr(VI)] from aqueous matrices with 74.11% efficiency (Ahmed 2017). A similar study using sawdust treated with NaOH and H_2SO_4 revealed efficient removal of heavy metals from aqueous solution: Cr(VI) (111.61 mg/g), Pb(II) (52.38 mg/g), Hg(II) (20.62 mg/g), and Cu(II) (5.64 mg/g) (Meena et al. 2008). Besides, Acacia sawdust successfully removed textile dyes from wastewater with an adsorption capacity of 267.04 mg/g onto basic sawdust acacia and 6.19 and 230.76 mg/g onto acidic sawdust acacia, respectively, for Brilliant Blue and Methylene Blue sorption (Tounsadi et al. 2020). Hence, the potential of waste Acacia sawdust can be explored to remove pharmaceutical products that are recently found in water bodies.

This study exploits the use of Acacia sawdust from the wood processing industry as a low-cost biomaterial to remove the NSAID compound, particularly IBP, from an aqueous solution. Specifically, it evaluated the efficiency of activated carbon from Acacia sawdust in removing IBP. Furthermore, the process was optimized; considering adsorption contact time, adsorbent dose, and initial IBP concentration; using the central composite design of Design Expert software. The adsorption mechanisms were investigated through isotherm and kinetic studies.

2 Materials and methods

2.1 Sawdust collection, acid modification, and carbonization

The Acacia sawdust was collected at the lumbering/sawmill industry in Misamis Oriental, Philippines. Such sawdust was dried at 105 °C and then, sieved to obtain a fine form (Oladimeji et al. 2021). Only particles of 40–60 mm diameter were used in the study.

Chosen dried sawdust was chemically modified by soaking in H_3PO_4 for 24 h in a 65% (v/v) concentration at room temperature. Afterward, the excess solution was removed, and the chemically modified sawdust was carbonized using a muffle furnace at 600 °C for 1 h (Oladimeji et al. 2021). The activated carbon was washed thoroughly with distilled water until pH 7 was reached. The washed activated carbon was then oven-dried at 105 °C for 12 h.

2.2 Analytical methods of Acacia sawdust properties

The moisture content of the as-received Acacia sawdust was determined using an oven. Four samples were dried in an oven at 105 °C. The mass of the sample was determined from time to time. On a dry basis, the moisture content was computed when there was no significant change in the mass of the sample. The density was determined by calculating the quotient of the mass and volume of the sample of Acacia sawdust. The as-received Acacia sawdust has a density of 26 kg/m^3 and a moisture content of 55.26 ± 4.62%.

The activated carbon from Acacia sawdust was analyzed using a scanning electron microscope (SEM) and Fourier-transformed infrared (FTIR) spectroscopy methods (Chakraborty et al. 2018), (Pagalan et al. 2020).

2.3 Preparation of Ibuprofen solution

Ibuprofen (IBP) was used as a contaminant in this study. The aqueous solution was made by dissolving Ibuprofen in distilled water at a predetermined dosage. Through a series of dilutions from a prepared 1000 ppm stock solution, the IBP concentration of each run, according to the design of the experiment, was prepared.

The efficiency (R) of activated carbon from Acacia sawdust in removing Ibuprofen in water was quantified using Eq. (1):

$$\text{ASAC removal efficiency}(R,\%) = \frac{C_o - C_f}{C_o} \times 100\% \quad (1)$$

where C_o and C_f are the initial and final equilibrium concentration (ppm) of Ibuprofen in the solution.

2.4 Parametric study and batch experiment

A calibration was first done by analyzing the absorbance of known concentrations of IBP (100–500 ppm). Such absorbances with their corresponding concentrations were plotted in a Cartesian plane using MS Excel, and the resulting trendline equation was used in computing the unknown concentration of IBP during preliminary and batch experiments. Simply, the absorbance (x) was inputted in the generated trendline equation ($y = mx + b$) to get the unknown IBP concentration (y).

The modeling of the removal of IBP contaminants was achieved by first doing preliminary runs, which were done before the batch experiment. In the preliminary runs, also known as parametric runs, the effects of each chosen variable were carefully studied independently. In this study, the chosen variables that have undergone a parametric study are initial Ibuprofen concentration (200–600 ppm), adsorbent dose (0.05–0.30 g), and contact time (20–70 min). These ranges of chosen variables' values are based on results of previous studies whereby optimum removal efficiencies were derived at these numbers.

After each run, the samples were filtered through a 0.45 µm membrane filter. The filtrate's absorbance with dissolved IBP was measured using a UV–Vis spectrophotometer set at 480 nm. An algorithm established from previously executed calibration experiments at known concentrations was used to calculate the residual IBP concentration.

The result of the parametric study became the basis of the design of the experiment using Design-Expert software. With this software and considering the data trend, experimental runs were generated considering the chosen variables in removing Ibuprofen, such as the effects of initial concentration, adsorbent dose, and contact time.

The experiment runs were carried out in a 250 mL Erlenmeyer flask with a working volume of 100 mL. The desired dose of activated carbon from Acacia sawdust was mixed in the aqueous solution with a predetermined IBP concentration. It was stirred using a magnetic stirrer according to a predetermined contact time based on the design of the experiment. All experimental results were entered into the Design-Expert program for statistical analysis and optimization.

After each run, the mixture was separated through filtration using filter paper. A UV–Vis spectrophotometer set at 480 nm wavelength determined the solution's absorbance. The residual Ibuprofen concentration was determined using the linear equation from the calibration curve firstly prepared for the purpose. After that, all the experiment results were entered into the Design Expert software for statistical analysis and optimization.

2.5 Statistical analysis

The experimental data were analyzed through analysis of variance that is built-in in the Design Expert software. It generated the best-fit response surface model; and the p values of variables (initial concentration, adsorbent dose, and contact time). The analysis was supplemented by rotatable 3D charts displaying 3D response surfaces.

The numerical optimization function of the central composite design using Design Expert software determined the most desirable solutions. Actual laboratory experiment runs were done to assess the combination of values of the chosen variables.

2.6 Isotherm and kinetic studies

The optimum conditions established through numerical optimization were used in the isotherm study, which was done according to classical methods such as Langmuir (Langmuir 1918) and Freundlich (Freundlich 1906). The optimum adsorbent dose and contact duration values were kept constant throughout the experiments, while the initial Ibuprofen concentration was the variable. Each run was replicated three times. Eq. (2) was used to examine the Langmuir isotherm, while Eq. (3) was employed in plotting Freundlich isotherm model:

$$\frac{1}{q_e} = \left[\frac{1}{bQ_O}\right]\frac{1}{C_e} + \frac{1}{Q_o} \tag{2}$$

$$\log q_e = \log K_f + \frac{1}{n}\log C_e \tag{3}$$

where Qe is the amount of adsorbate adsorbed per unit mass of adsorbent (mg/g), Qo is the adsorption capacity (mg/g), b is the energy of adsorption (L/mg), Ce is the equilibrium concentration of the adsorbate (mg/L), Kf is the Freundlich capacity factor, and $1/n$ is the intensity variable.

The kinetic study was based on optimum conditions established using variable contact time. Like another study (de Luna et al. 2017), the experimental data, in triplicate, were used for first- and second-pseudo-order kinetics. The first-order and second-order kinetic equations are shown in Eqs. (4 & 5)

$$InC_t = InC_o - k_1 t \tag{4}$$

$$\frac{1}{C_t} = \frac{1}{C_o} + k_2 t \tag{5}$$

where C_0 is the initial concentration of Ibuprofen (g/L), C_t is the concentration of reaction time (mg/L), t is the contact time (min), K_1 is the first-order rate constant (h^{-1}), and K_2 is the rate constant of second-order (min/L).

3 Results and discussion

3.1 Characteristics of carbonized Acacia sawdust

Activated carbon's surface structure and pore distribution from Acacia sawdust were determined using scanning electron microscopy or SEM (Fig. 1). The analysis showed that the activation process using H_3PO_4 caused modification of the structures of Acacia sawdust by burning its particles, resulting in numerous pores on the adsorbent. It is also observed in another study showing the same characteristics (Ahmad et al. 2020a, b). A similar study using coconut husk activated carbon revealed a successful removal of IBP with evidence that such compound stuck onto the pores of the adsorbent (Solomon et al. 2020). This result is likewise observed in the removal of IBP using ASAC, whereby the IBP compound was trapped in the adsorbent (Fig. 1b). As observed, the ASAC is surrounded by numerous small particles, most likely IBP. It implied that IBP removal using ASAC was successful as the micropores accommodated the IBP compound and permanently stuck onto the surface.

The functional groups on the surface of the ASAC are primarily responsible for the IBP adhesion that occurs via adsorption (Chakraborty and Halder 2020). Like in Fig. 2, the FTIR analysis enables one to make accurate predictions about the presence of functional groups on the surface of sorbents before and after IBP adhesion (Wahab et al. 2010). The identified bands of the FTIR spectra are presented in Table 1. The peak at 3327 cm^{-1} and 3359 cm^{-1} indicated the O–H stretching of the bonded hydroxyl groups. It is an indication that alcohol is present in ASAC. The same result was found in the previous study, whereby -OH groups were found in 3470 cm^{-1} (Li et al. 2017) and 3336 cm^{-1} (Zhu et al. 2009) of the surface of activated carbon.

Asymmetry was observed at 2197 cm^{-1} and 2202 cm^{-1} due to the stretching of numerous bonds (–N=C=O asym. stretch) and the stretching of nitrogen bonds. This result implied that the ASAC adsorbent has a possible composition of cyanide, isocyanate, and thiocyanate (Tran et al. 2021). This outcome postulated that nitrogen molecules may have bonded to the ASAC surface at 2300–1990 cm^{-1} (Coates and Ed 2000), and numerous bond chemistries have accumulated. At 1984.24 $cm^{-1}$and 1959.29 cm^{-1}, there was a clear indication of C-O stretching consisting of oxygenated groups such as alcohol, phenols, and ethers. It showed that such oxygenated compounds with C–O stretching are present on the ASAC surface.

The notable C–H stretch was seen in 1750–1680 cm^{-1}, indicating a carboxylic acid group. Particularly, the detected peak of 1689.13 cm^{-1} in the spent ASAC only indicated the presence of the carboxylic acid group. Such a band can be ascribed to propionic acid (Guedidi et al. 2017), which in this study is Ibuprofen. This peculiar band is expected because of the deposition of Ibuprofen (propionic acid) in the matrices of ASAC during adsorption. This outcome that can be observed only in the spent ASAC manifested the physical attachment of IBP onto the ASAC during adsorption.

The C=C stretch, observed at 1560.02 cm^{-1} and 1557.56 cm^{-1}, suggests the presence of aromatic groups. Previous work reported the same findings whereby 1575 cm^{-1} was ascribed to aromatic C=C stretching vibrations (Tran et al. 2021). The -SO_3 stretch band due to ether groups at 1300–1000 cm^{-1} occurred at 1276.21 cm^{-1} and 1290.16 cm^{-1}, indicating the presence of silanol. This band relates to surface silanol's H-bonded

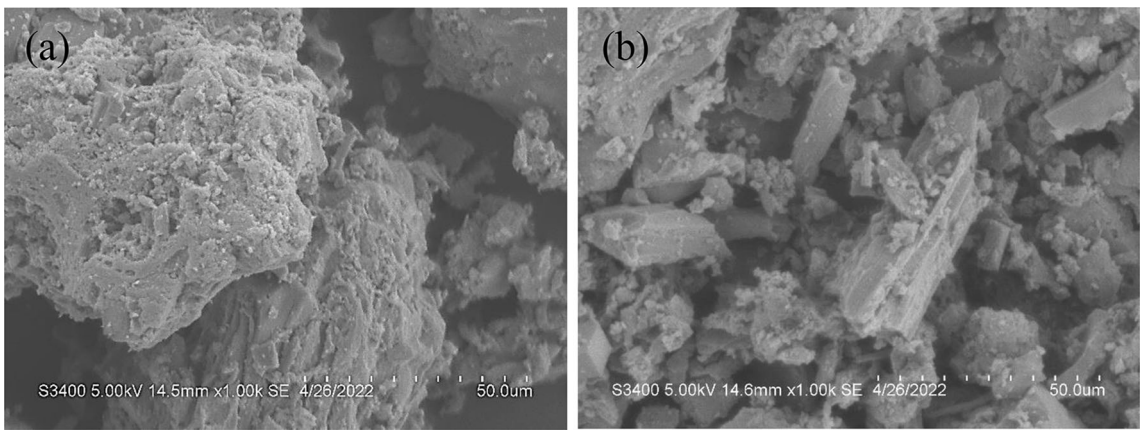

Fig. 1 SEM images of **a** pristine, and **b** spent ASAC

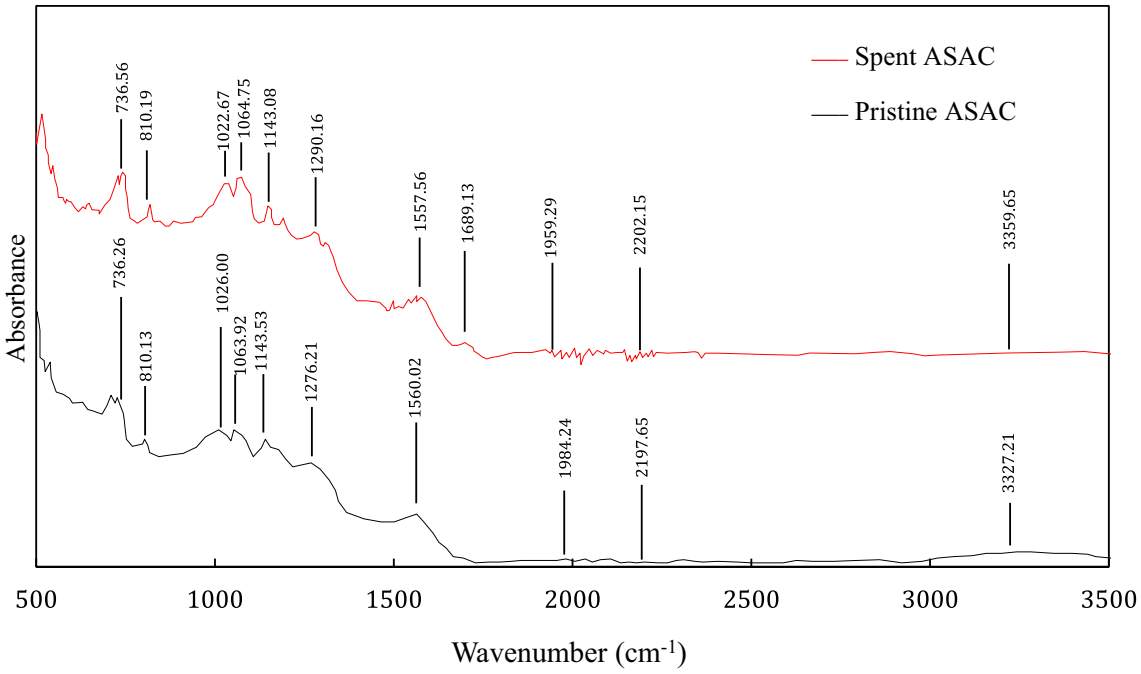

Fig. 2 FTIR spectra of **a**) pristine and **b** spent ASAC

Table 1 FTIR spectral characteristics of ASAC before and after adsorption

Wavelength range (cm^{-1})	Acacia sawdust activated carbon (cm^{-1})		Band	Assignment
	pristine (before)	Spent (After)		
3500–3200	3327.21	3359.65	O–H stretch	Alcohol (bonded hydroxyl groups)
2200–2000	2197.65	2202.15	–N=C=O asym. stretch	Isocyanate, cyanide ion, thiocynate ion, and related ions
2000–1650	1984.24	1959.29	C-O stretch	Oxygenated groups (alcohol, phenols, ethers)
1750–1680	Absent	1689.13	C-H stretch	Carboxylic acid (propionic acid, Ibuprofen)
1640–1500	1560.02	1557.56	C=C stretch	Aromatics
1300–1000	1276.21	1290.16	$–SO_3$ strech	Silanol
1350–1000	1143.53	1143.08	O–H	Alcohols (primary and secondary) and aliphatic ethers
1150–1000	1063.92	1064.75	C–O stretch	Alcohol, phenols, ethers
	1026.00	1022.67		
860–800	810.13	810.19	C–H out-of-plane bending	Aromatic including alcohol
800–700	736.26	736.56	C–H out-of-plane vibration	Alkene

Si–O stretching mode (Tripp and Hair 1993), and 1132 cm^{-1} or 1035 cm^{-1} as Si–O-Si stretching (Airoldi and Alcântara 1995). The O–H deformation was found within 1300–1000 cm^{-1}, indicating the existence of hydroxyl groups. The actual peaks were observed at 1143.53 cm^{-1} and 1143.08 cm^{-1}, ascribing the presence of alcohols (primary and secondary) and aliphatic ethers. This observation was also reported in another study postulating that 1050 cm^{-1} and 1200 cm^{-1} vibrations can be attributed to alcohols, phenols, acids, or esters (Zheng et al. 2014; Sun et al. 2015).

The C-O stretch, which can be used to determine whether alcohol groups are present, was observed in 1150 cm^{-1} and 1000 cm^{-1}. Actual peaks were found in 1063.92 cm^{-1}, 1064.75 cm^{-1}, 1026.00 cm^{-1}, and 1022.67 cm^{-1}, indicating the presence of ethers, phenols,

and alcohol. As described in the previous works, the band in this range, like 1028 cm^{-1}, can be attributed to the elongation vibration of C–O bonds in alcohols, phenols, and ethers (Li et al. 2020; Oba et al. 2021b). The presence of an aromatic group can be observed from the peaks found in the band between 860 and 800 cm^{-1}. The actual peaks at 810.13 cm^{-1} and 810.19 cm^{-1} indicated that ASAC contains aromatics, including alcohol. This result is supported by the previous finding, stating that the bands at 875–750 cm^{-1} were attributed to aromatic C–H out-of-plane bending vibrations, suggesting the occurrence of aromatization (including alcohol condensation and dehydration (Li et al. 2017). An out-of-plane C–H vibration bond was observed at 736.26 cm^{-1} and 736.56 cm^{-1}, signifying the presence of alkenes in ASAC. The same finding was articulated in a prior study, with 786 cm^{-1} and 707 cm^{-1} peaks corresponding to alkenes' C–H bending vibrations (Caglayan and Aksoylu 2013).

Overall, the identified functional bands of O–H, C–O, and COOH groups provide sites for interaction for hydrogen bonding between ASAC and IBP. In contrast, the aromatic regions indicated by the C–C stretch enable interaction via π-stacking (Omorogie et al. 2021). This means that Van der Waals and hydrogen bonding interactions with the carboxylic groups of IBP were mediated by oxygeneous functional groups. The ASAC's oxygeneous functional groups (such as carbonyl, phenolic, and others) can form a donor–acceptor contact with IBP's aromatic ring [16]. The mechanism of IBP adsorption, in the case of adsorbents containing an H-donor functional group (–OH), can be based on the complexation between a hydrogen bond and an anionic IBP conjugate (H-acceptor) [13]. Additionally, any lone pair of oxygen electrons on an oxygenated ASAC adsorbent can form donor–acceptor complexes via a dipole moment with IBP molecules. In effect, such carbonyl groups of stronger dipole moment donated the electron, which can be accepted by the IBP aromatic ring (Mattson et al. 1969). These interactions are fundamental for binding IBP onto ASAC, which is responsible for the good IBP adsorption capacity.

3.2 Optimization of experimental conditions

At variable adsorbent dose (0.05–0.30 g), the removal percentage increases from 44.4 to 91.1% (Fig. 3). An increase in adsorbent dose provided additional active sites for adsorbates to occupy. According to a study of date stone biochar for sorptive removal of Ibuprofen, most of the unoccupied active site was initially accessible, resulting in IBP distribution to the unrestricted active site of the adsorbents' surface area (Chakraborty et al. 2020). The removal of IBP that peaked at 91.1% suggested that 0.30 g ASAC would serve as the main basis in the range of the

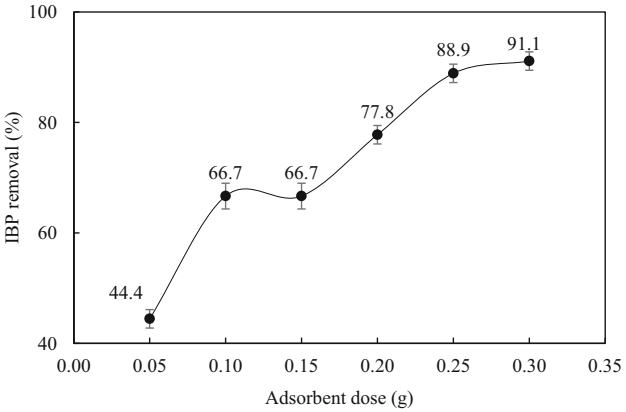

Fig. 3 Ibuprofen removal rate at a variable ASAC adsorbent dose (Constant: 60 min contact time, 300 IBP initial concentration)

mass of adsorbent dose when designing the experiment for batch adsorption of IBP.

At variable contact times (20—70 min), the removal of IBP increases as the contact time also increases from 66.7% to 88.9% (Fig. 4). Based on the trend of the IBP removal rate using ASAC at variable contact time, it can be implied that IBP can best be removed at 50–70 min. The same was used as the basis in the design of the experiment for batch adsorption of IBP.

At variable initial IBP concentrations (200–600 ppm), there is an increasing trend of IBP removal from 83.3 to 94.4% (Fig. 5). Because more IBP surrounds the active sites of the produced ASAC adsorbent in the solution at higher initial concentrations, the steadiness of the adsorption capacity of activated carbon increases as the IBP concentrations increase, thereby improving the adsorption activities. In the related study of the removal of diclofenac using Isabel grape bagasse, published elsewhere, similar effects of diclofenac initial concentration to removal rate were found whereby dosage from 15 to 30 mg/L resulted in a shorter equilibrium period (100 to 80 min), with elimination percentages ranging from 16.4 to 22.8 (de Luna et al. 2017). It further postulated that the interaction

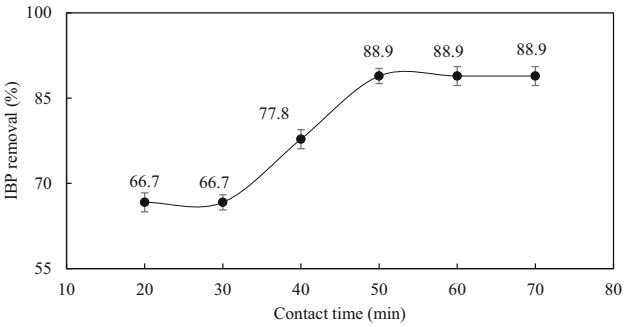

Fig. 4 Ibuprofen removal rate at variable contact time (Constant: 0.25 g ASAC adsorbent dose, 300 IBP initial concentration)

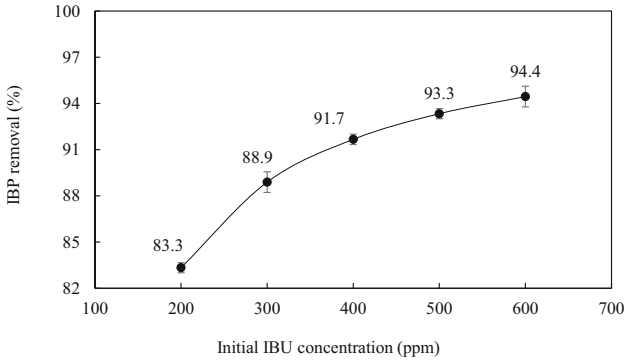

Fig. 5 Ibuprofen removal rate at variable initial IBP concentration (Constant: 0.25 g ASAC adsorbent dose, 50 min contact time)

between the adsorbent and the adsorbate was increased as the concentration was raised, resulting in larger removal percentages. The initial study's findings at different IBP concentrations suggested that removal rates are rising even at higher concentrations, with a 94.4% removal rate at 600 ppm—the basis of the design of the experiment.

3.3 Efficiency of Acacia sawdust activated carbon in the removal of IBP

Through optimization of experimental conditions, the 0.25 g adsorbent dose, 50 min contact time, and 500 ppm of IBP initial concentration were considered as the center points (coded level 0) in the making of the design of the experiment using the central composite design of the response surface methodology (Table 2). With these chosen factors, 20 runs were generated, ready for batch experimentation to determine the efficiency of Acacia sawdust activated carbon in removing Ibuprofen.

The batch experiments were conducted following the CCD experimental design (Table 3). It was discovered that the ASAC effectively removed Ibuprofen from aqueous solutions between 72.22 and 100%. These findings revealed that the interplay of the operating variables impacts ASAC's Ibuprofen removal efficiency.

Table 4 shows that Ibuprofen removal using ASAC can be reliably simulated (p value = 0.0001). The Prob > F is also significant, with only a 0.01% chance of error when using ASAC to predict the percentage removal of IBP from an aqueous solution. Using the generated quadratic equation, the results were 99.99% reliable and precise in predicting the desired outcome value of percent IBP removal. A p value of 0.9399 for a non-significant lack of fit indicated that the data were well-fit and the model developed was reliable. Moreover, the model's R^2 value of 0.9399 supported the claim that the model equation, Eq. (6), could estimate the percentage of Ibuprofen removed using ASAC.

$$y = 236.51649 - 980.36538A + 0.63978B - 0.18691C + 1.38887AB + 1.66665AC - 0.00138887BC + 305.19175A^2 - 0.000703456B^2 - 0.000193541C^2 \quad (6)$$

Considering the algebraic signs of the terms of the equation, the positive sign of B means increasing the contact duration independently of IBP and ASAC in an aqueous solution, resulting in a higher percent removal. On the other hand, the negative coefficient of ASAC adsorbent dose (A) and initial IBP concentration (C) could independently reduce the removal efficiency. Only the interaction of AC (p value = 0.0001) can be statistically explained as having substantial impacts among the three interacting variables (AB, AC, and BC). Increasing the numeric coefficient of AC would lead to an increased percent removal of Ibuprofen. Additionally, the term C^2 with a negative numerical coefficient is significant (p value = 0.0067), indicating the reduction in the removal rate of Ibuprofen from the aqueous solution using ASAC.

Table 2 Experimental range and level of independent factor

Factor	Coded level				
	− 2	− 1	0	1	2
Adsorbent dose (g)	0.15	0.20	0.25	0.30	0.35
Contact time (min)	30	40	50	60	70
IBP initial concentration (ppm)	300	400	500	600	700

3.4 Interactive effects of the significant variables in the removal of IBP using ASAC

According to Fig. 6, the increase in ASAC dose at high IBP concentration showed an increasing trend in the aqueous solution's removal percentage. More adsorbent means more active sites for the IBP and ASAC to interact, leading to the sticking of IBP onto ASAC surfaces. At lower IBP concentrations, the percent removal is generally high. This observation can be attributed to successful adsorption, considering that low concentration means the available active sites of ASAC successfully accommodated a few IBP particles in the solution. A study also shows a similar effect of the interaction with initial concentration and adsorbent dose in *Prosopis juliflora* activated carbon (PJAC) whereby adsorptive uptake of ofloxacin indicated that, at low PJAC dosage, the percentage uptake was less. However, as the PJAC dose was increased, the proportion of ofloxacin uptake gradually increased up to some point and eventually decreased thereafter (Kaur et al. 2022). Additionally, the availability of more ofloxacin explained

Table 3 Result of the batch experiment of Ibuprofen removal using ASAC

Run	Adsorbent dose (g)	Contact time (min)	Initial IBP concentration (ppm)	Removal (%)
1	0.35	50	500	100.00
2	0.20	60	400	100.00
3	0.30	40	400	83.33
4	0.25	50	500	93.33
5	0.30	60	400	91.67
6	0.15	50	500	86.67
7	0.25	50	700	76.19
8	0.25	50	300	88.89
9	0.25	50	500	93.33
10	0.20	40	600	72.22
11	0.20	60	600	72.22
12	0.25	50	500	86.67
13	0.25	30	500	86.67
14	0.25	50	500	93.33
15	0.25	70	500	93.33
16	0.30	40	600	94.44
17	0.25	50	500	86.67
18	0.25	50	500	86.67
19	0.20	40	400	91.67
20	0.30	60	600	100.00

Table 4 Analysis of variance of the removal of Ibuprofen using Acacia sawdust activated carbon

Source	Sum of squares	df	Mean Square	*F* Value	*p* value Prob > F
Model	1186.797	9	131.8663	16.23844	< 0.0001[a]
A-ASAC Adsorbent dose (g)	224.9955	1	224.9955	27.70666	0.0004[a]
B-Contact time (min)	79.01077	1	79.01077	9.729636	0.0109[a]
C-Initial IBP concentration (ppm)	176.7176	1	176.7176	21.76157	0.0009[a]
AB	3.857948	1	3.857948	0.47508	0.5063[b]
AC	555.5444	1	555.5444	68.41151	< 0.0001[a]
BC	15.43179	1	15.43179	1.90032	0.1981[b]
A^2	14.6366	1	14.6366	1.802397	0.2091[b]
B^2	0.12442	1	0.12442	0.015321	0.9039[b]
C^2	94.18006	1	94.18006	11.59763	0.0067[a]
Residual	81.20629	10	8.120629		
Lack of Fit	14.54095	5	2.908191	0.218119	0.9399[b]
Pure Error	66.66533	5	13.33307		
Cor Total	1268.003	19			
R^2 = 0.9399					

a=significant; b=not significant

the variance in the removal rate's increasing trend with concentration.

3.5 Result of numerical optimization

According to the optimization outcome generated by the software using the batch experiment data, the best conditions that would result in an optimum theoretical IBP yield of 99.39% are at 0.20 g adsorbent dose, 60 min contact time, 400 ppm initial IBP concentration (Table 5). The actual result shows 98.61 ± 1.39% IBP removal in an aqueous solution with a percent error of 0.78% from the theoretical value. The predicted 99.39% and an actual 98.61 ± 1.39% IBP removal rates were significantly close.

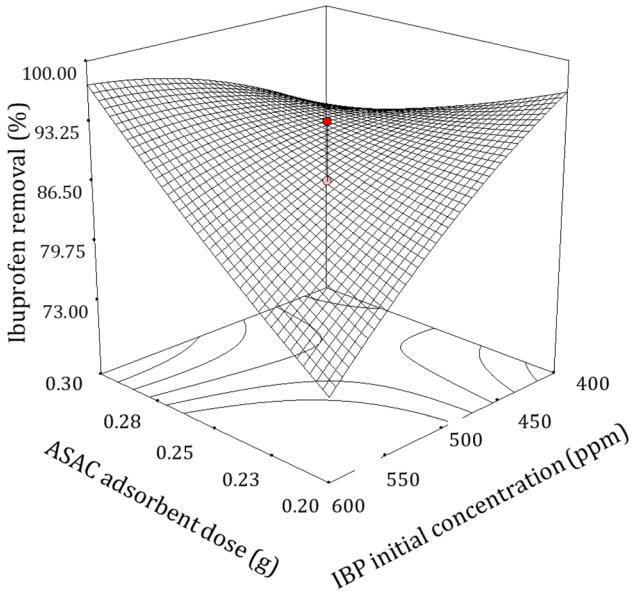

Fig. 6 Effect of adsorbent dose and initial dose of Ibuprofen removal by Acacia sawdust activated carbon

3.6 Isotherm and kinetic modeling

The interaction between IBP and ASAC via adsorption was investigated via an isotherm study employing a constant adsorbent dose of 0.20 g, contact time of 60 min, and variable IBP concentrations of 300, 400, 500, 600 and 700 ppm.

The result showed that the Langmuir model provided the best fit in explaining the adsorption mechanism between IBP and ASAC with an R^2 value of 0.9787, way higher than the R^2 of 0.8446 of the Freundlich model (Fig. 7). This finding suggested that the adsorption mechanism was monolayer adsorption on the surface of the homogeneously organized adsorbent (Priyantha et al. 2015; Aurich et al. 2017). The IBP molecules stick onto the surface of the ASAC in a single layer, implying that a greater volume of ASAC adsorbent would result in higher IBP adsorption efficiency. A review on the removal of IBP via numerous adsorbents also showed Langmuir model as the best-fitted isotherm that explained the removal of IBP (Oba et al. 2021a).

The isotherm constants of the two isotherm models are shown in Table 6. With the most fitted Langmuir model, the adsorption capacity of ASAC achieved an adsorption capacity of 121.95 mg/g. A gram of ASAC can efficiently remove 121.95 mg of IBP in an aqueous solution.

The result is a little lower than the IBP adsorption uptake using rice husk acid-AC (239.8 mg/g) but got better adsorption efficiency than palm shell AC (100.6 mg/g), activated coco husk (76.92 mg/g), unmodified palm shell AC (72.70 mg/g), acid-functionalized bean husk (50.0 mg/g), pinewood biochar (10.74 mg/g) and activated apple wood biochar (2.50 mg/g) (Table 7). Therefore, the ASAC brings a huge potential for activated carbon production with a higher ability to remove IBP from an aqueous solution.

The most appropriate kinetic model was determined by conducting experimental kinetic runs under the optimum conditions of the initial IBP concentration of 400 ppm, adsorbent dose of 0.20 g, and variable contact time (30–70 min). Figure 8 illustrates the results of the experimental runs of the kinetic model analysis with corresponding kinetic constants shown in Table 8.

The results showed that the pseudo-first-order was the fittest model for IBP uptake from aqueous solution via adsorption with a correlation coefficient (R^2) of 0.9863, way better than R^2 of 0.2275 for the pseudo-second-order model. There is strong evidence that physisorption took place, and it also shows that diffusion was in charge of the adsorption process while the experiment was conducted (Simonin 2016). The type of reaction is directly related to the concentration of the reactants (Baek et al. 2010). Similar research employing rape straw biomass fiber/-CD/Fe_3O_4 as an adsorbent in removing IBP discovered that hydrogen bond forces and electrostatic interaction are involved in the adsorption process, suggesting that physisorption is crucial in the removal of IBP (Wu et al. 2021). This work can be interpreted by saying that IBP removal using ASAC happened through the physical bonding of IBP molecules onto the surface of ASAC through Van der Waals forces. Like the study using waste coffee residue in removing IBP, it can be concluded that adsorption progressed spontaneously and endothermically and was mainly controlled by the pore-filling effect, hydrogen bonding, and π–π EDA interaction (Shin et al. 2021).

Table 5 Optimum conditions to efficiently remove Ibuprofen using Acacia sawdust activated carbon

Particular	Adsorbent dose (g)	Contact time (min)	Initial IBP concentration (ppm)	IBP Removal (%)
CCD	0.20	60	400	99.39
Actual	0.20	60	400	98.61 ± 1.39

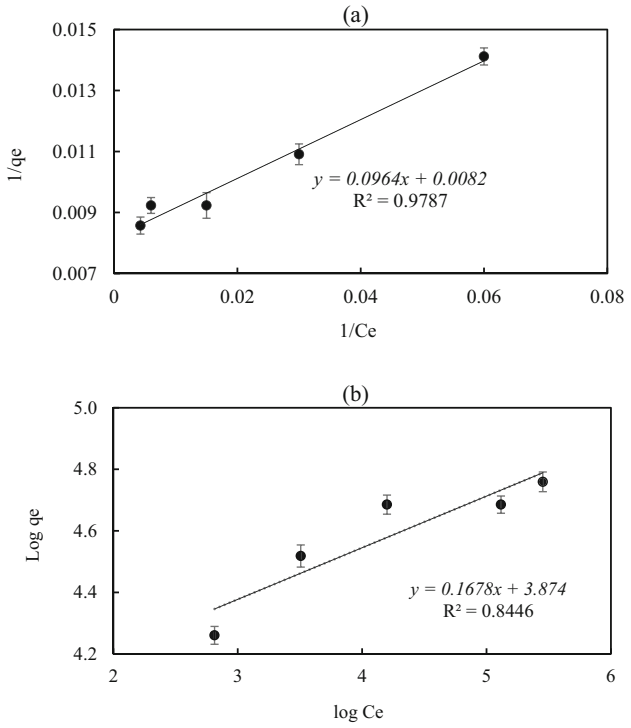

Fig. 7 Isotherm analysis result using **a** Langmuir model, **b** Freundlich in the removal of IBP using ASAC

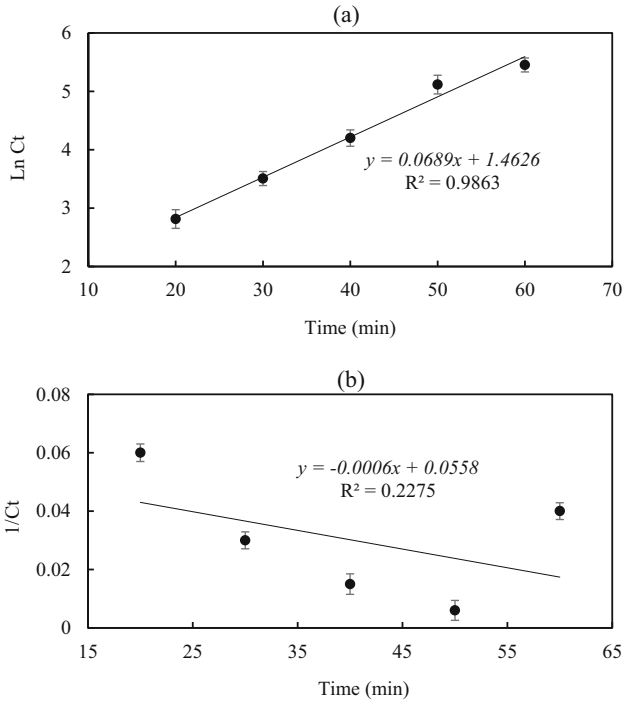

Fig. 8 Kinetic models showing **a** pseudo-first-order, and **b** pseudo-second order in the removal of IBP using ASAC

Table 6 Isotherm constants and correlation coefficients

Isotherm	Parameter	Value	R^2
Langmuir	Energy of adsorption, b(L/mg)	0.085062	0.9787
	Adsorption capacity, Q_o(mg/g)	121.95	
Freundlich	Empirical parameter, $1/n$	0.1678	0.8446
	Freundlich constant,K_f	0.588	

Table 8 Kinetic model constants and correlation coefficients in the removal of IBP using ASAC

Kinetic model	Constant	Value	R^2
1st order	LnC_o(mg/L)	1.4626	0.9863
	K_1(1/min)	0.0689	
2nd order	$1/C_o$(mg/L)	0.0558	0.2275
	K_2(min/L)	0.0006	

Table 7 Adsorption capacities of different organic adsorbents for aqueous IBP uptake

Adsorbent	Qo_{max},(mg/g)	Reference
Acacia sawdust AC	121.95	This study
Rice husk acid-AC	239.8	(Álvarez-Torrellas et al. 2016)
Palm shell AC modified with 3.8% Fe	157.3	(Tiek Wong et al. 2015)
Palm shell AC modified with 7.8% Fe	100.6	(Wong et al. 2016)
Activated coconut husk	76.92	(Solomon et al. 2020)
Unmodified palm shell AC	72.70	(Tiek Wong et al. 2015)
Acid-functionalized bean husk	50.00	(Bello et al. 2019)
Activated wood apple biochar	12.66	(Chakraborty et al. 2018)
Pinewood biochar	10.74	(Essandoh et al. 2015)
Wood apple biochar	2.50	(Chakraborty et al. 2018)

4 Conclusion

The use of waste Acacia sawdust from the wood processing industry has been exploited and proven to be among the low-cost biomaterial in the removal of Ibuprofen, a non-steroidal anti-inflammatory drug that is found in water bodies as a pollutant. The Acacia sawdust is a promising precursor in producing Acacia sawdust activated carbon (ASAC) to remove Ibuprofen and may be other NSAIDs in an aqueous solution. With H_3PO_4, the Acacia sawdust was chemically modified, with ASAC showing better pore structures desirable for adsorption. The IBP adsorption onto ASAC was successful because the functional groups, such as O–H, C–O, and COOH, reacted in various ways. Compared to other activated carbons employed in removing IBP, the results revealed a high adsorption capacity of 121.95 mg/g. Because of the active adsorption sites, the IBP removal rate is high at high ASAC dosages. More ASAC results in more elimination of the IBP compound since IBP was linked to the ASAC active sites in a monolayer (Langmuir isotherm). The physical adsorption (physisorption) explained how the adsorption mechanism removed IBP using ASAC (pseudo-first-order kinetics).

Acknowledgements The authors would like to thank the faculty of the College of Engineering and Technology of the University of Science and Technology of Southern Philippines—Claveria (USTP Claveria) for their support. The laboratory analyses were provided by Pilipinas Kao, Incorporated, which the authors gratefully acknowledge.

Author contributions All authors have contributed to the study from conceptualization, laboratory experimentation, data gathering, analysis, and interpretation. All authors read and approved the final manuscript.

Funding This work is institutionally funded by the University of Science and Technology of Southern Philippines.

Availability of data and materials All data generated or analyzed during this study can be available upon request. If needed, you may contact the corresponding author for a soft copy of the data.

Declarations

Conflict of interest The authors declare that they have no conflict of interest.

References

Ahmad MA, Mohamad Yusop MF, Zakaria R, Karim J, Yahaya NK, Mohamed Yusoff MA, Fazlin Hashim NH, Abdullah NS (2020a) Adsorption of methylene blue from aqueous solution by peanut shell based activated carbon. Mater Today Proc 47:1246–1251. https://doi.org/10.1016/j.matpr.2021.02.789

Ahmad AA, Mohd Din AT, Yahaya NK, Karim J, Ahmad MA (2020b) Atenolol sequestration using activated carbon derived from gasified Glyricidia sepium. Arab J Chem 13:7544–7557. https://doi.org/10.1016/j.arabjc.2020.08.029

Ahmed MJ (2017) Adsorption of non-steroidal anti-inflammatory drugs from aqueous solution using activated carbons: Review. J Environ Manage 190:274–282. https://doi.org/10.1016/j.jenvman.2016.12.073

Airoldi C, Alcântara EFC (1995) Chemisorption of divalent cations on N-(2-pyridyl)acetamide immobilized on silica gel - A thermodynamic study. J Chem Thermodyn 27:623–632. https://doi.org/10.1006/jcht.1995.0064

Álvarez-Torrellas S, Rodríguez A, Ovejero G, García J (2016) Comparative adsorption performance of ibuprofen and tetracycline from aqueous solution by carbonaceous materials. Chem Eng J 283:936–947. https://doi.org/10.1016/j.cej.2015.08.023

Aurich A, Hofmann J, Oltrogge R, Wecks M, Gläser R, Blömer L, Mauersberger S, Müller RA, Sicker D, Giannis A (2017) Improved isolation of microbiologically produced (2R,3S)-isocitric acid by adsorption on activated carbon and recovery with methanol. Org Process Res Dev 21:866–870. https://doi.org/10.1021/acs.oprd.7b00090

Baek MH, Ijagbemi CO, Kim DS (2010) Removal of malachite green from aqueous solution using degreased coffee bean. J Hazard Mater 176:820–828. https://doi.org/10.1016/j.jhazmat.2009.11.110

Bello OS, Alao OC, Alagbada TC, Olatunde AM (2019) Biosorption of ibuprofen using functionalized bean husks. Sustain Chem Pharm 13:100151. https://doi.org/10.1016/j.scp.2019.100151

Caglayan BS, Aksoylu AE (2013) CO_2 adsorption on chemically modified activated carbon. J Hazard Mater 252–253:19–28. https://doi.org/10.1016/j.jhazmat.2013.02.028

Chakraborty P, Halder G (2020) Ibuprofen sorptive efficacy of zirconium caged date seed derived steam activated alginate beads in a static bed column. RSC Adv 10:24293–24307. https://doi.org/10.1039/d0ra04265j

Chakraborty P, Banerjee S, Kumar S, Sadhukhan S, Halder G (2018) Elucidation of ibuprofen uptake capability of raw and steam activated biochar of aegle marmelos shell: isotherm, kinetics, thermodynamics and cost estimation. Proc Safety Envi Prot 118:10–13. https://doi.org/10.1016/j.psep.2018.06.015

Chakraborty P, Singh SD, Gorai I, Singh D, Rahman WU (2020) Explication of physically and chemically treated date stone biochar for sorptive remotion of ibuprofen from aqueous solution. J Water Process Eng 33:101022. https://doi.org/10.1016/j.jwpe.2019.101022

Chopra S, Kumar D (2020) Ibuprofen as an emerging organic contaminant in environment, distribution and remediation. Heliyon 6:e04087. https://doi.org/10.1016/j.heliyon.2020.e04087

de Luna MD, Murniati BW, Rivera KK, Arazo R (2017) Removal of sodium diclofenac from aqueous solution by adsorbents derived from cocoa pod husks. J Environ Chem Eng 5:1465–1474. https://doi.org/10.1016/j.jece.2017.02.018

Essandoh M, Kunwar B, Pittman CU, Mohan D, Mlsna D (2015) Sorptive removal of salicylic acid and ibuprofen from aqueous solutions using pine wood fast pyrolysis biochar. Chem Eng J 265:219–227. https://doi.org/10.1016/j.cej.2014.12.006

Freundlich FHM (1906) Over the adsorption in solution. J Phys Chem 57:1100–1107

Guedidi H, Reinert L, Soneda Y, Bellakhal N, Duclaux L (2017) Adsorption of ibuprofen from aqueous solution on chemically surface-modified activated carbon cloths. Arab J Chem 10:S3584–S3594. https://doi.org/10.1016/j.arabjc.2014.03.007

Coates J, Ed RAM (2000) Interpretation of infrared spectra, a practical approach. 10815–10837

Jamoussi B, Chakroun R, Jablaoui C, Rhazi L (2020) Efficiency of Acacia gummifera powder as biosorbent for simultaneous

decontamination of water polluted with metals. Arab J Chem 13:7459–7481. https://doi.org/10.1016/j.arabjc.2020.08.022
Kaur G, Singh N, Rajor A (2022) RSM-CCD optimized Prosopis juliflora activated carbon for the adsorptive uptake of Ofloxacin and disposal studies. Environ Technol Innov 25:102176. https://doi.org/10.1016/j.eti.2021.102176
Langmuir I (1918) Adsorption of gases on plane surfaces of glass, mica, and platinum. J Am Chem Soc 40:1361–1403. https://doi.org/10.1021/ja02242a004
Li S, Liang F, Wang J, Zhang H, Zhang S (2017) Preparation of mono-dispersed carbonaceous spheres via a hydrothermal process. Adv Powder Technol 28:2648–2657. https://doi.org/10.1016/j.apt.2017.07.017
Li Z, Hanafy H, Zhang L, Sellaoui L, Netto MS, Oliveira MLS, Seliem MK, Dotto GL, Bonilla-Petriciolet A, Li Q (2020) Adsorption of congo red and methylene blue dyes on an ashitaba waste and a walnut shell-based activated carbon from aqueous solutions: experiments, characterization and physical interpretations. Chem Eng J 388:124263. https://doi.org/10.1016/j.cej.2020.124263
Mattson JS, Mark HB, Malbin MD, Weber WJ, Crittenden JC (1969) Surface chemistry of active carbon: specific adsorption of phenols. J Colloid Interface Sci 31:116–130. https://doi.org/10.1016/0021-9797(69)90089-7
Meena AK, Kadirvelu K, Mishra GK, Rajagopal C, Nagar PN (2008) Adsorptive removal of heavy metals from aqueous solution by treated sawdust (Acacia arabica). J Hazard Mater 150:604–611. https://doi.org/10.1016/j.jhazmat.2007.05.030
Oba SN, Ighalo JO, Aniagor CO, Adaobi C (2021) Removal of ibuprofen from aqueous media by adsorption: a comprehensive review. Sci Total Environ 780:146608. https://doi.org/10.1016/j.scitotenv.2021.146608
Oladimeji TE, Odunoye BO, Elehinafe FB, Oyinlola OR, Olayemi OA (2021) Production of activated carbon from sawdust and its efficiency in the treatment of sewage water. Heliyon 7:e05960. https://doi.org/10.1016/j.heliyon.2021.e05960
Omorogie MO, Babalola JO, Ismaeel MO, McGettrick JD, Watson TM, Dawson DM, Carta M, Kuehnel MF (2021) Activated carbon from Nauclea diderrichii agricultural waste – a promising adsorbent for ibuprofen, methylene blue and CO_2. Adv Powder Technol 32:866–874. https://doi.org/10.1016/j.apt.2021.01.031
Pagalan E, Sebron M, Gomez S, Salva SJ, Ampusta R, Macarayo AJ, Joyno C, Ido A, Arazo R (2020) Activated carbon from spent coffee grounds as an adsorbent for treatment of water contaminated by aniline yellow dye. Ind Crop Prod 145:111953. https://doi.org/10.1016/j.indcrop.2019.111953
Phasuphan W, Praphairaksit N, Imyim A (2019) Removal of ibuprofen, diclofenac, and naproxen from water using chitosan-modified waste tire crumb rubber. J Mol Liq 294:111554. https://doi.org/10.1016/j.molliq.2019.111554
Priyantha N, Lim LBL, Dahri MK (2015) Dragon fruit skin as a potential biosorbent for the removal of methylene blue dye from aqueous solution. Int Food Res J 22:2141–2148. https://doi.org/10.1136/bmj.326.7401.0-d
Rakic V, Rac V, Krmar M, Otman O, Auroux A (2014) The adsorption of pharmaceutically active compounds from aqueous solutions onto activated carbons. J Hazard Mater 282:141–149. https://doi.org/10.1016/j.jhazmat.2014.04.062
Shin J, Kwak J, Kim S, Son C, Lee YG, Baek S, Park Y, Chae KJ, Yang E, Chon K (2021) Facilitated physisorption of ibuprofen on waste coffee residue biochars through simultaneous magnetization and activation in groundwater and lake water: adsorption mechanisms and reusability. J Environ Chem Eng Preproof: https://doi.org/10.1016/j.jece.2022.107914
Simonin J (2016) On the comparison of pseudo-first order and pseudo-second order rate laws in the modeling of adsorption kinetics. Chem Eng J 300:254–263. https://doi.org/10.1016/j.cej.2016.04.079
Solomon O, Abiola M, Adenike B, Christianah I (2020) Ibuprofen removal using coconut husk activated biomass. Chem Data Collect 29:100533. https://doi.org/10.1016/j.cdc.2020.100533
Souza HdO, Costa RdS, Quadra GR, Fernandez AdS (2021) Pharmaceutical pollution and sustainable development goals: going the right way? Sustain Chem Pharm 21:100428. https://doi.org/10.1016/j.scp.2021.100428
Sun YG, Ma YL, Wang LQ, Wang FZ, Wu QQ, Pan GY (2015) Physicochemical properties of corn stalk after treatment using steam explosion coupled with acid or alkali. Carbohydr Polym 117:486–493. https://doi.org/10.1016/j.carbpol.2014.09.066
Tiek Wong K, Yoon Y, Jang M (2015) Enhanced recyclable magnetized palm shell waste-based powdered activated carbon for the removal of ibuprofen: Insights for kinetics and mechanisms. PLoS ONE 10:1–18. https://doi.org/10.1371/journal.pone.0141013
Tounsadi H, Metarfi Y, Barka N, Taleb M, Rais Z (2020) Removal of textile dyes by chemically treated sawdust of Acacia: Kinetic and equilibrium studies. J Chem 2020:1–12. https://doi.org/10.1155/2020/7234218
Tran TH, Le HH, Pham TH, Nguyen DT, La DD, Chang SW, Lee SM, Chung WJ, Nguyen DD (2021) Comparative study on methylene blue adsorption behavior of coffee husk-derived activated carbon materials prepared using hydrothermal and soaking methods. J Environ Chem Eng 9:105362. https://doi.org/10.1016/j.jece.2021.105362
Tripp CP, Hair ML (1993) Chemical attachment of chlorosilanes to silica: a two-step amine-promoted reaction. J Phys Chem 97:5693–5698. https://doi.org/10.1021/j100123a038
Wahab MA, Jellali S, Jedidi N (2010) Ammonium biosorption onto sawdust: FTIR analysis, kinetics and adsorption isotherms modeling. Bioresour Technol 101:5070–5075. https://doi.org/10.1016/j.biortech.2010.01.121
Wang J, Yang F (2020) Preparation of 2-hydroxypropyl-b-cyclodextrin polymers crosslinked by poly (acrylic acid) for efficient removal of ibuprofen. Mater Lett 284:128882. https://doi.org/10.1016/j.matlet.2020.128882
Wong KT, Yoon Y, Snyder SA, Jang M (2016) Phenyl-functionalized magnetic palm-based powdered activated carbon for the effective removal of selected pharmaceutical and endocrine-disruptive compounds. Chemosphere 152:71–80. https://doi.org/10.1016/j.chemosphere.2016.02.090
Wu G, Liu Q, Wang J, Xia S, Wu H, Zong J, Han J, Xing W (2021) Facile fabrication of rape straw biomass fiber/β-CD/Fe_3O_4 as adsorbent for effective removal of ibuprofen. Ind Crops Prod 173:114150. https://doi.org/10.1016/j.indcrop.2021.114150
Yang Q, Huang H, Li K, Wang Y, Wang J, Zhang X (2021) Ibuprofen removal from drinking water by electro-peroxone in carbon cloth filter. Chem Eng J 415:127618. https://doi.org/10.1016/j.cej.2020.127618
Zheng J, Zhao Q, Ye Z (2014) Preparation and characterization of activated carbon fiber (ACF) from cotton woven waste. Appl Surf Sci 299:86–91. https://doi.org/10.1016/j.apsusc.2014.01.190
Zhu J, Yang J, Deng B (2009) Enhanced mercury ion adsorption by amine-modified activated carbon. J Hazard Mater 166:866–872. https://doi.org/10.1016/j.jhazmat.2008.11.095